

# EARTH SCIENCE SYSTEM STUDY

## TROPOSPHERIC OZONE FABRY-PEROT INTERFEROMETER

### FINAL REPORT

William A. Roettker, NASA Langley Research Center

#### OBJECTIVES

The purpose of the Tropospheric Ozone Fabry-Perot Interferometer (TO3FPI) System Study is to develop a conceptual instrument design that defines the technical requirements of major components of a compact, space-based, high spectral resolution sensor for measuring tropospheric ozone based upon Fabry-Perot interferometry. These components may include detectors, optical elements, high-precision actuators, electronic and data processing segments, coolers, and structural components. Using the results of the conceptual instrument studies, the system study will identify technologies required to enable instrument development and improve scientific return, reduce spacecraft resource requirements (power, mass, data storage and transmission, etc.), and lower life cycle costs. Finally, the system study will provide an estimate of the resources required to advance the technologies identified above to a technology readiness level (TRL) of 6 (system/subsystem model or prototype demonstration in a relevant ground or space environment).

The three objectives of the TO3FPI System Study are to:

1. Develop conceptual instrument design and technical requirements for a space-based tropospheric ozone Fabry-Perot interferometer (FPI).
2. Identify critical technologies needed to enable the instrument concept.
3. Estimate resources required to advance critical technologies to TRL 6.

#### SCIENCE RATIONALE

Space-based observation of tropospheric chemistry is one of the high-priority atmospheric science measurements to be included in Earth science missions of the 21st century, and is included as one of the key measurement areas identified in the NASA Office of Earth Science (OES) Strategic Enterprise Plan. The objective of the Tropospheric Ozone Fabry-Perot Interferometer (TO3FPI) is the direct measurement of tropospheric ozone from space, which fits directly within the OES Atmospheric Ozone measurement theme.

Levels of tropospheric ozone have been increasing and will continue to increase as concentrations of the precursor gases (oxides of nitrogen, methane, and other hydrocarbons) necessary for the photochemical formation of tropospheric ozone continue to rise. In fact, there is evidence suggesting that average surface ozone concentrations may have doubled over the last century [Volz and Kley, 1988]. In addition, the discovery of enhanced tropospheric ozone over the south tropical Atlantic Ocean [Fishman et al, 1990] shows that the problem is not unique to urban areas. It is becoming well known that exposure to enhanced levels of tropospheric ozone adversely impacts health, crops, vegetation, and climate.

A global tropospheric ozone monitoring capability is critical to enhancing scientific understanding and potentially lessening the ill-health impacts associated with exposure to elevated concentrations in the lower atmosphere. However, challenges associated with this measurement have prevented the development of such a remote sensing device. Current practice is to infer tropospheric residuals [Fishman et al, 1990] by subtracting stratospheric ozone amounts from total ozone: a small difference of two large numbers from two independent non-collocated satellite sensors, both of which contain measurement uncertainty. The long-term goal of this effort is to enable "direct" observation of tropospheric ozone from a space-based platform.

#### MEASUREMENT DESCRIPTION

Earlier NASA-sponsored work [Larar, 1993] has shown that a tropospheric ozone measurement capability can be achieved using a satellite-based nadir-viewing device making high spectral resolution measurements with high signal-to-noise ratios, and that a Fabry-Perot interferometer (FPI) is quite suitable for this task. A satellite-based, passive sensor provides a global monitoring capability with low power consumption relative to active techniques. The nadir-viewing configuration will enable high horizontal spatial resolution desired for tropospheric trace species monitoring while minimizing cloud interference. Implementation in the infrared portion of the spectrum utilizes the strong 9.6-micron ozone band and yields continuous day/night coverage independent of solar zenith angle. An FPI affords high optical throughput while operating at high spectral resolution, and has a

proven success record in previous space-based applications.

Molecular collisions during the absorption/emission process give rise to collisional or pressure broadening, and the corresponding profile function can be represented by the Lorentz line shape. The Lorentz half-width is proportional to pressure and is approximately inversely proportional to the square root of temperature. The other significant mechanism for broadening in the terrestrial atmosphere is Doppler broadening, which originates from a Doppler shift in the frequency of radiation associated with the absorption/emission feature due to thermal motion of the radiating molecules. Unlike the Lorentzian half-width, the Doppler half-width does not have a pressure dependence and therefore its change with altitude is due to temperature alone. The Voigt profile is formed from the convolution of two independent broadening formulas (i.e., Lorentzian and Doppler) and in the high or low pressure limits approaches the Lorentz or Doppler profiles, respectively. Figure 1 illustrates the approximate Lorentz, Doppler, and Voigt half-widths as a function of altitude for ozone lines within the 9.6 micron band (using reasonable surface values for the Lorentz and Doppler half-widths [Kuhn and London, 1969] and Lorentz half-width temperature dependence coefficient [Rothman et al, 1987]). The figure illustrates the basis for this measurement concept: tropospheric information content in the measured signals can be maximized by spectrally isolating wings of strong ozone lines, since wings of strong lines are due primarily to pressure broadening in the troposphere.

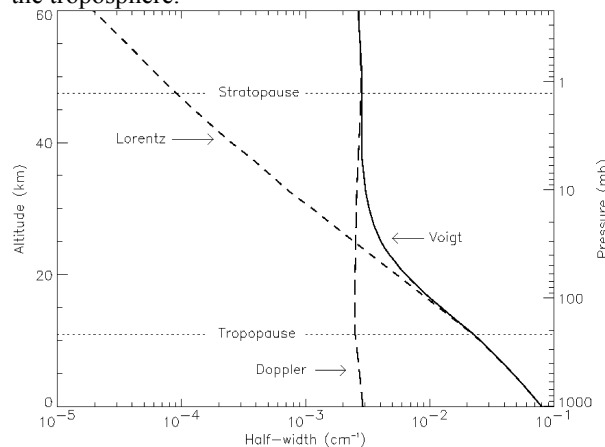


**Figure 1.** Approximate altitude dependence from 0 to 60 km of Lorentz, Doppler, and Voigt half-widths.

## MEASUREMENT CONCEPT

The TO3FPI instrument concept employs a double-etalon FPI for high-resolution, narrow-band infrared emission measurements within the strong 9.6-micron ozone band. Such an implementation requires a

single-order transmission function, rather than the periodic nature of the standard Fabry-Perot instrument bandpass (which can be advantageous when observation of periodic spectra is desired). This can be achieved with additional optical elements to reduce the effect of unwanted passbands, improve sideband rejection, and extend the effective free spectral range. Figure 2 summarizes the formation of a single-order, double-etalon instrumental transfer function from the Airy (A), defect (D), aperture (L), and bandpass filter (T<sub>F</sub>) functions.

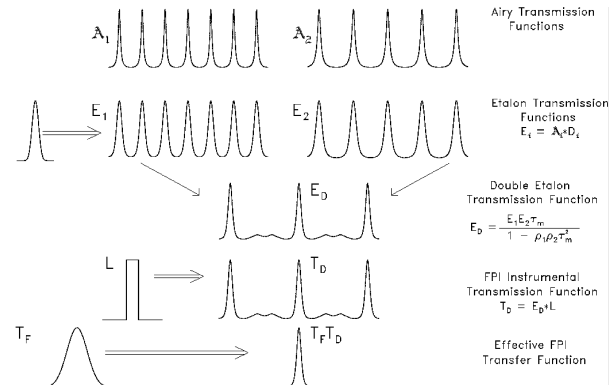


**Figure 2.** Schematic diagram summarizing the formation of a single-order, double-etalon instrumental transfer function.

This instrument concept involves a double-etalon fixed-gap series configuration FPI along with an ultra-narrow bandpass filter to achieve single-order operation with an overall spectral resolution of approximately  $0.068 \text{ cm}^{-1}$  [Larar et al, 1998]. The new Circle to Line Interferometer Optical (CLIO) system [Hays, 1990] (U.S. patent #4893003, 1990) accomplishes the spatial scanning of the fringe plane, and thus enables multi-channel operation (simultaneous observation of multiple spectral channels of information). This approach has significant advantages over conventional scanning techniques: the need for mechanical scanning is eliminated, and it provides a signal multiplex advantage by detecting all the energy in the imaged ring pattern. In addition, a longer dwell time per spectral channel may be achieved since all channels are measured simultaneously; this is of particular interest for satellite applications where the instrument field-of-view (FOV) is in motion relative to the target scene. A successful laboratory demonstration of the CLIO system has been carried out at the University of Michigan's Space Physics Research Laboratory (UM/SPRL) [Hays, 1990]. In addition, the CLIO system has been included as a vital ingredient in the Multi-Order Etalon Sounder (MOES) instrument design concept [Wang, 1990].

The basic optical configuration of this instrument concept using the CLIO system is illustrated in Figure 3. The basis behind this instrument is to combine high throughput and resolution capabilities of an FPI with single-order transmission characteristics of a double-etalon configuration along with maximizing signal-to-noise ratio (SNR) qualities of the CLIO system to achieve spectral isolation capabilities while minimizing the impact of undesirable signal contributions (e.g., interferant species, surface, etc.). Through proper selection of channel spectral regions, an FPI optimized for tropospheric ozone measurements can simultaneously observe a stratospheric component and thus the total ozone column abundance. Spectral channels are defined by the spatial distribution of detector elements within a detector array.

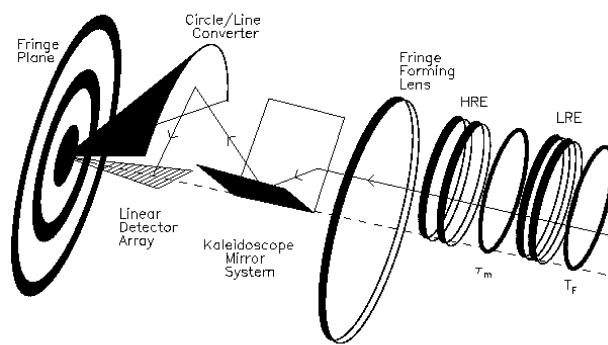


**Figure 3.** Basic optical configuration of a double-etalon FPI, showing the relative placement of key optical elements.

The feasibility of tropospheric and total ozone observations from a space-based platform using a double-etalon FPI has been addressed in an earlier study [Larar and Drayson, 1998]. Simulations indicate vertical discrimination capability between tropospheric and stratospheric ozone fields using the proposed instrumentation, supporting the threshold minimum measurement performance of obtaining integrated column amounts for both the troposphere and stratosphere. However, the measurement goal of some profiling capability also appears achievable since an averaging kernel analysis has shown that approximately seven independent pieces of vertical information should be obtainable for this ozone retrieval, with roughly three located in the troposphere. This analysis also estimated the achievable vertical resolution to decrease with altitude and range from  $\sim 6$  km near the surface to  $\sim 8$  km in the upper troposphere and from  $\sim 8$  km to  $\sim 11$  km in the stratosphere. An error analysis, which considered the impact on retrieved integrated ozone amounts from the most significant uncertainties associated with this particular measurement, showed the proposed instrumentation to enable a good measurement of absolute ozone amounts and an even

better determination of relative changes. Expectations are that this technique can enable integrated tropospheric ozone determination to within  $\sim 10\%$  precision and  $\sim 20\%$  accuracy, and knowledge of total column ozone abundance to within  $\sim 4\%$  precision and  $\sim 5\%$  accuracy. While further studies are still to be performed, current results support preliminary feasibility of this space-based measurement and these estimates compare quite favorably with the capabilities of the limited number of instruments/techniques that are currently making (or are planned to make) similar observations.

Two possible science mission scenarios centered about this FPI are currently envisioned: 1) a dedicated tropospheric ozone measurement, where complimentary sensors would be included only as needed to improve the ozone retrieval (i.e., to provide temperature,  $H_2O$ , and surface information), or 2) a broader tropospheric chemistry package, which would include additional sensors to also measure other key chemical species (eg.  $NO_x$ ,  $CO$ ,  $CH_4$ , and other hydrocarbons). Both measurement objectives can be accomplished with this Fabry-Perot interferometry technology used in conjunction with a lower-resolution Fourier Transform Spectrometer (FTS) of currently available technology. Simultaneous measurements using a low-resolution FTS will enable temperature and water vapor profiles along with surface characteristics (i.e., temperature and emissivity) to be implemented into the TO3FPI ozone retrieval; additionally, a lower-resolution observation of the entire ozone band will be available for cross-calibration verification.

## INSTRUMENT SYSTEM CONCEPT

An instrument system concept has been developed for a double-etalon FPI combined with a low-resolution FTS placed in a 950-km circular orbit [Bremer et al 1998]. The FPI segment provides high spectral resolution measurements of atmospheric constituents of interest (e.g. ozone). The lower resolution FTS provides temperature, water vapor, and surface information required for the ozone retrieval. Both science segments share an input telescope and collimating mirrors to guarantee spatial co-registration. A beamsplitter directs energy to each of the science segments: the FPI double etalons and the FTS single-pass Michelson scanning interferometer configured with corner cube retro-reflectors and three spectral bands.

### Optical Design

The primary design goal for TO3FPI was maximizing radiometric performance while keeping an eye on feasibility of fabrication and alignment, and minimizing mass and volume. Refractive elements were minimized to maintain performance over the wide spectral range and to minimize weight and transmission

losses. All powered elements are reflective to prevent the introduction of chromatic aberrations. When dealing with a high-performance, wide field-of-view system, component size and spacing will tend to grow large, making packaging difficult. Figure 4 shows an overview of the instrument optical design illuminated by full field-of-view light bundles. For clarity, the CLIO focal plane packages are not shown.

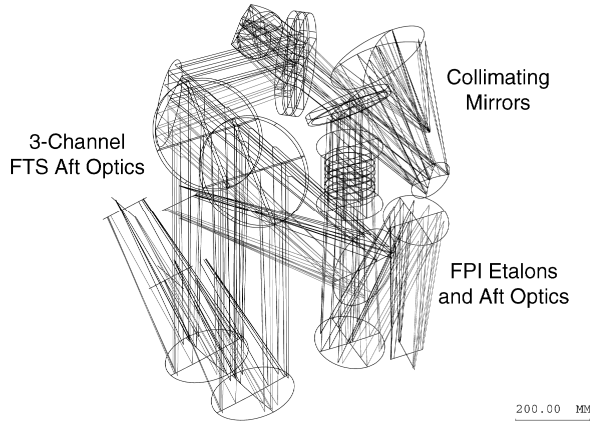


**Figure 4.** Optical design of the TO3FPI instrument concept.

The primary mirror is a 229-mm diameter off-axis conical mirror. The image of the mirror is accepted into the beam scrambler, a hollow cylinder reflective on the inside whose entrance is the system field stop. The beam scrambler mixes light from the FOV so that its output is an integration of the total energy. Two mirrors collimate the output of the scrambler to a 130-mm diameter beam (1.8x magnification). Collimated light from the beam scrambler is separated by a beamsplitter that reflects the narrow ozone spectral band to the FPI segment. The FPI utilizes dual etalons tuned in multiples of free spectral range. The output of both is close to the free spectral range of the lower resolution etalon combined with the narrow bandpass of the high-resolution etalon.

Light not reflected into the FPI is passed into the Michelson interferometer. Once the light enters the interferometer, it is ideally split 50/50 on the partially reflective back surface of the zinc selenide beamsplitter plate. The reflection coating is a dielectric material with an index higher than ZnSe. This assures equal beam phases in both arms, producing constructive interference at zero path difference (ZPD). The compensator plate (used for dispersion equalization) is placed immediately behind the beamsplitter plate. Using the beamsplitter and compensator back-to-back allows a more compact interferometer. Both plates are wedged slightly to prevent ghost fringes due to interference with the reflections off the other 3 surfaces. A single-pass interferometer is necessary due to the

wide field of view of the system. A longer path multi-pass interferometer length would cause excessive beam growth and require very large optics in both the interferometer and the focus groups. The pupil is placed directly in front of each arm's retroreflectors where matching Lyot stops are located. This maximizes the interferometer's acceptance of collimated light and equalizes the beams in the two arms. The Michelson mirrors are hollow corner cube (3-mirror) retroreflectors. This makes the interferometer insensitive to tilt (a difficult parameter to maintain) while scanning, but doubles the sensitivity to shear.

Light exiting the interferometer is split into three spectral bands centered around carbon dioxide, water, and ozone using dichroic dielectric coatings on two ZnSe Plates. Each dichroic beamsplitter reflects the shorter IR wavelength band and passes the longer wavelengths. Each individual channel has its own focusing optics, CLIO, and detector array. Note that light leaving the Michelson interferometer expands quickly (by 5.4 degrees). A powered fold mirror is utilized to prevent beam growth while passing through the aft beamsplitters to the focal optics. Each of the three focal planes is rotated out of plane to be easily accessible by the cryogenic cooling system.

## Radiometric Analysis

A radiometric analysis of the baseline instrument was performed to evaluate the potential performance of the FPI. SNRs were calculated assuming a detectivity ( $D^*$ ) of  $2.5 \times 10^{12}$ , a one-second dwell time, and optics temperatures ranging from 200 to 300 K. Calculated values of SNR indicated that the FPI should have an adequate SNR even with dwell times much less than one second [Bremer et al 1998].

## Sensitivity Analysis

The purpose of a sensitivity analysis is to define the first-order sensitivities of the instrument to mechanical stability. Several figures of merit have been considered in the error-budgeting process, but since the requirements on instrument performance are undetermined, the budgets and tolerances presented here are preliminary. This sensitivity analysis is only for component stability and does not cover fabrication and alignment.

Two figures of merit have been simultaneously considered in the sensitivity analysis: line scan function (LSF) and boresight error. LSF is evaluated in only one axis, along the direction of the pixel array. In addition, the LSF is evaluated at the extreme angle of light coming through the interferometer. This allows a single data 'point' to be used in the analyses. Since LSF is dependent on both diffraction and geometric aberrations, the quadrant overlaying function of the CLIO must be included in the evaluation. Boresight

error is an additional quantity to control. Boresight error is defined as the shift which a predetermined chief ray makes from its nominal position, and can be understood in either of two equivalent ways: as a shift of the image away from its nominal position on the detector, measured in linear units (mm); and as a change in the pointing direction of the instrument measured in angular units (mrad) in object space. For components following the telescope image, the limit will be set by the requirement on channel co-registration.

Telescope perturbations will not affect this internal constraint, but instead will ‘move’ the FOV about in object space. This is one component to the boresight constraint requirement on the pointing knowledge of the entire instrument. These budgets have not yet been determined.

All components, except the interferometers, are subject to the minimum stability requirements given in Table 1. These values are for alignments relative to other components with the same group. Large “bulk” movements are acceptable given changes maintain co-registration of the channels.

**Table 1.** Baseline component stability

Component	Decenter (mm)	Focus (mm)	Tip/Tilt (mrad)	Rotation (mrad)
Powered mirrors	0.02	0.01	0.05	0.01
Flats/beam splitter	0.5	0.5	0.05	5
Focus components	0.04	0.02	0.05	0.1

Because the system is not diffraction limited, we are not able to perform a more detailed analysis of each sensitivity. The baseline stabilities given in Table 1 are all within achievable limits and do not further degrade the baseline system. What this implies is that the focusing systems are stable in imaging performance, if the baseline performance is acceptable. If we increase requirements and design a higher-performance system, there would be a need for a detailed sensitivity study.

## Mechanical Design

A conceptual mechanical design of the TO3FPI instrument incorporating optical mirrors, lenses, optical bench, and electronics has been developed (Figures 5 and 6). This design is based on a kinematically mounted optical bench with an aluminum core and graphite facesheets. FPI and FTS optical components are mounted on both sides of the optical bench using “traditional” mount materials and techniques (aluminum mirrors, ZnSe transmissive elements, and titanium brackets). The estimated mass of this system is nearly 200 kg; when a growth margin of 40% is

included, the total mass approaches 275 kg [Bremer et al 1998]. This large mass estimate is based on current practice for instrument design, and offers the best opportunity for the infusion of new technologies such as lightweight optics and optical benches; small, efficient actuators; and composite structures.

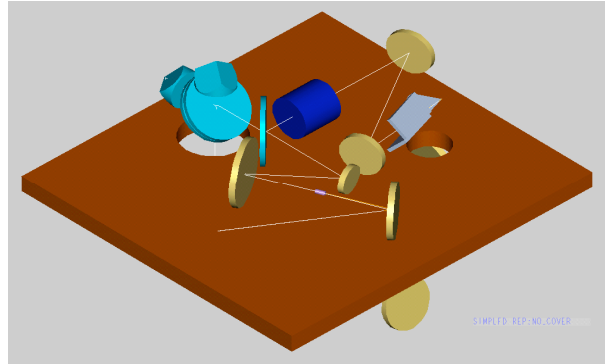


**Figure 5.** Isometric top view of optical layout of TO3FPI instrument concept.

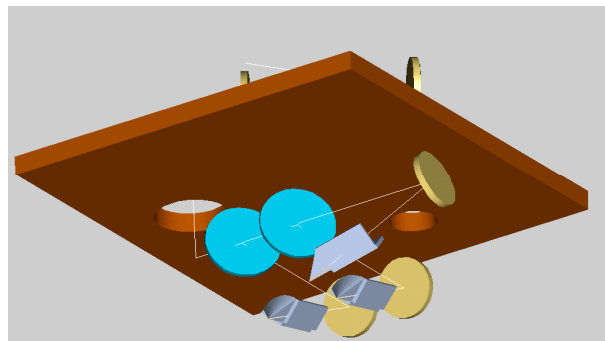


**Figure 6.** Isometric bottom view of optical layout of TO3FPI instrument concept.

Mechanisms are required to provide for fine adjustment of the FPI etalons and for translation of the FTS moving mirror. The etalon mechanism must adjust position in response to error signals from an alignment laser and maintain etalon position with little or no power. The FTS mechanism must translate the mirror at a constant 2.15 cm/sec velocity over a 1-cm stroke.

## Thermal Design

The primary goal for the TO3FPI conceptual thermal design is to maintain the FPI and FTS detectors at their required temperatures. The preliminary temperature requirements are 80 K for the FPI detectors and 55 K for the FTS detectors. The optical bench is cooled to approximately 200 K to reduce the instrument background on the IR detectors. The TO3FPI thermal control concept is illustrated in Figure 7. Advanced technologies discussed later in this report can reduce the complexity and mass of the thermal control system.

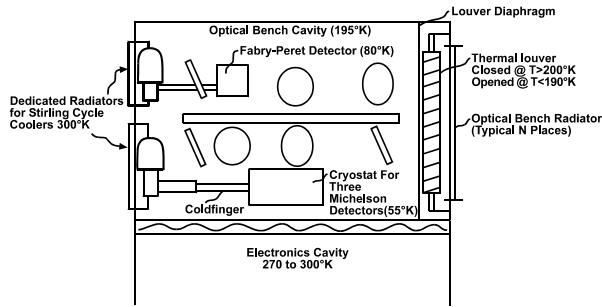


**Figure 7.** Thermal control concept for the TO3FPI instrument.

One of two methods could be used to achieve the required detector temperatures: a mechanical cryogenic cooler or a stored cryogen dewar. A stored cryogen dewar would require up to 1000 kg of cryogen (such as liquid nitrogen) to attain a three year mission life. Mechanical coolers would have a mass of approximately 15 kg each and would require 50-150 watts of electrical power to cool the detectors to required temperatures.

## TECHNOLOGY ASSESSMENT

While a feasible instrument concept using currently available technology can be developed, the spacecraft resources required to maintain the instrument are quite considerable. The instrument concept described above using currently available technology would weigh at least several hundred kilograms and consume several hundred watts of electrical power. To enable the instrument concept in a compact, lightweight, low-power space-based sensor, several enabling technologies have been identified that require advancement beyond current technology readiness levels (TRLs). Incorporating these advanced technologies has the potential to reduce the instrument mass to 50 kg or less, and consume less than 50 watts of power.

For each of the technologies discussed below, an evaluation of the current TRL is provided, and an estimate of the resources required to advance to TRL 6 is given. The maturity of the technologies is based on the technology readiness levels listed in Table 2.

**Table 2.** Technology Readiness Levels (TRL)

<b>TRL 1</b>	Basic principles observed and reported
<b>TRL 2</b>	Technology concept and/or application formulated
<b>TRL 3</b>	Analytical and experimental critical function and/or characteristic proof-of-concept
<b>TRL 4</b>	Component and/or breadboard validation in laboratory environment
<b>TRL 5</b>	Component and/or breadboard validation in relevant environment
<b>TRL 6</b>	System/subsystem model or prototype demonstration in a relevant environment (ground or space)
<b>TRL 7</b>	System prototype demonstration in a space environment
<b>TRL 8</b>	Actual system completed and “flight qualified” through test and demonstration (ground or space)
<b>TRL 9</b>	Actual system “flight proven” through successful mission operations

## Precision etalon control

A key feature of the proposed measurement concept is the optical performance and spectral tuning of the FPI. NASA LaRC’s R&T program has initiated development of a unique and compact system for controlling the spacing and parallelism between two mirrors. This technique was conceived and patented several years ago. A system containing low voltage piezoelectric actuators, solid-state stable frequency lasers and patented angle interferometers can produce a small, low power system that allows optimum performance and versatility for a space-based Fabry-Perot interferometer.

The system to control Fabry-Perot etalon mirrors includes sensors to detect the distance and the deviation angle from parallel between the mirrors. In addition, the system requires appropriate actuators for setting the separation and maintaining parallelism between the mirrors. These same technologies, in different configurations, are also applicable to other Earth and space science instruments.

In order to sense the distance between the mirrors and the angle between them, a stable frequency laser will be utilized. This laser is all solid state for high reliability and is based on the Pound-Drever-Hall technique that locks a laser frequency to the resonance of a high finesse cavity. The laser will be miniaturized and designed for long life in the space environment. This laser will be the basis for a heterodyne interferometer with sub-nanometer displacement resolution. The same laser, combined with an angle interferometer about the size of a sugar cube, will detect

the angle between the mirrors with sub-arcsecond resolution using only a single beam reflected from each mirror. This is a significant advantage over conventional systems that require three beams to make this measurement. In order to scan the mirrors and maintain the parallelism finesse, it is necessary to actuate the mirrors. To accomplish this function a revolutionary new material actuator will be used. Based on several patents, the thin-layer composite unimorph ferroelectric driver and sensor, or THUNDER, is a piezoelectric device with about 1000 times the displacement potential of conventional PZT's. This allows a low voltage implementation of the mirror actuator that saves mass, power and volume over conventional PZT actuators.

While each of the components of the precision etalon control system has been developed and demonstrated, the components must be integrated into an operational system to validate its performance and demonstrate volume, mass, and power requirements. The combination of several new technological developments allows an extremely efficient, compact and low mass Fabry-Perot mirror spacing and parallelism control system to be achieved.

*Current TRL: 4*

*Resources to reach TRL 6: 1 year, \$200K*

### **High sensitivity two-dimensional infrared detector arrays**

Another key feature of the proposed measurement concept is the use of a passively cooled infrared detector array with sensitivity comparable to that of conventional detectors cooled to 77 K. These detectors are based on mercury-manganese-telluride (HgMnTe), a material system developed in part under the NASA LaRC R&T program. Researchers at the Massachusetts Institute of Technology and Brimrose Corporation have collaborated with NASA LaRC to develop this technology in both single detector and array format. Initial tests over a range of temperatures indicate that D\*'s can be achieved at temperatures just over 100 K which meet the sensitivity requirements for the detection of tropospheric ozone from space.

Infrared detector technology must be advanced by expanding the size of the array format to 128 x 128 and higher, and by developing a technique for reliable and efficient read-out electronics fabrication and integration with the detector array. Larger array formats can enable additional measurement opportunities; for example, a geostationary imaging capability.

Advancing detector array technology is technically challenging and can be expensive. Excellent progress has been made with HgMnTe in the past several years using Sensor and Detector Technology Program funding. Further investments to advance this

technology's readiness promise large payoffs for many future measurement concepts.

*Current TRL: 4*

*Resources to reach TRL 6: 2 years, \$2.5M*

### **High efficiency passive thermal control**

To achieve the sensitivity required to make atmospheric chemistry measurements from space, current infrared sensors rely on high-sensitivity detectors cooled to cryogenic temperatures (55-77 K). Typically, these temperatures are achieved using stored cryogens (such as liquid nitrogen) or active cryocoolers (such as Stirling cycle coolers). To meet mission lifetimes of one year or more, stored cryogen systems must be large and massive. Stored cryogens also pose difficult ground and launch processing problems. Active coolers can also be large and heavy, and require large amounts of power to cool to cryogenic temperatures. Long-term reliability of cryocoolers has been a difficult problem to address. By combining several technologies, including improved thermal isolation techniques, advanced passive thermal radiators, and high-sensitivity infrared detectors described above, future infrared remote sensors could avoid the use of stored cryogens and active coolers.

Electrochromic devices, if fully developed, could replace the mechanical thermal louvers that are shown in the baseline design. These devices provide controllable broadband (UV and IR) reflectance through the application of low voltage, using conducting polymer (CP) technology. By using a  $\pm 1.2$ -volt power supply with a 1 to 2 milliamp pulse width, emissivities between 0.30 and 0.67 have been obtained. If the emissivity range could be expanded to (0.10 to 0.90), then electrochromic devices could replace louvers and perhaps variable conductance heatpipes (VCHP).

By combining advancements in several technology areas, particularly high sensitivity infrared detectors, the goal of a passively cooled infrared sensor is within reach. If detectors with sufficient sensitivity can be demonstrated to operate at 100 K, the integration of innovative thermal isolation techniques, such as fiber-supported focal planes, with new flat panel radiative coolers can be demonstrated fairly easily. High efficiency passive thermal control simply requires the integration of the advancements of other technologies currently being advanced.

*Current TRL: 2*

*Resources to reach TRL 6: 1 year, \$500,000 after demonstration of precursor technologies.*

### **Cryogenic Devices**

There are several cryogenic devices requiring further development that would optimize the design, reduce the risk, and maximize the lifetime of TO3FPI.

These devices include cryogenic thermal switches, cryogenic thermal storage units and cryogenic thermal transport systems.

**Cryogenic Thermal Switches.** Due to lack of statistical life test data on long-life mechanical cryocoolers, cryogenic thermal switches are required to enable redundant cryocoolers to be incorporated into the system. The resulting system would have two cryocoolers for each detector: an operating cryocooler and a redundant, non-operating cryocooler. Each cryocooler would be configured with a cryogenic thermal switch in the thermal path between it (the cryocooler) and the detector.

Another potential application for a cryogenic thermal switch would be to open or close the thermal path from a variable temperature cooling source (e.g., the optical bench radiator) to a cryogenic thermal storage unit (described below) in order to maximize the thermal storage unit performance. This type of thermal switch needs to be able to turn on and off very quickly (that is, in a matter of minutes) in order to match the variation in temperature of the cooling source.

At present, there are no flight-proven cryogenic thermal switches that can turn on and off quickly. The concepts that offer the most potential include a gas-gap/hydride pump thermal switch, a differential CTE thermal switch, a pressure-actuated bellows cryogenic thermal switch, and a cryogenic capillary pumped loop (described below in the thermal transport device section). Except for the cryogenic capillary pumped loop, conceptual designs for these potential cryogenic thermal switch options are available, but no fully-functioning units been built.

*Current TRL: 3*

*Resources to reach TRL 6: 3 years, \$750,000.*

**Cryogenic Thermal Storage Units.** A thermal storage unit stores and releases heat at a constant temperature. Due to the variable heat load on the optical bench radiator (even with a thermal louver or a variable emittance coating), the radiator must be large enough so that its average temperature is acceptably low. Time-varying parasitic heat loads on the detectors might also increase the heat-lift requirements on the cryocoolers. A cryogenic thermal storage unit (CTSU) can equalize these variable heat loads and temperatures.

High-performance CTSUs, especially those operating at 60 K and below, are dual-volume devices with an ambient storage tank and a cryogenic heat exchanger. A small tube connects the two volumes. The system is filled with a fluid (typically a gas at ambient temperature) that changes phase slightly below the operating temperature of the cooled component (radiator or detector). At present, a nitrogen triple-point (63.15 K) CTSU has been flight qualified as part of the CRYOTSU flight experiment on STS-95. A nitrogen trifluoride (NF<sub>3</sub>)-based CTSU that utilizes the NF<sub>3</sub>

solid-solid transition at 56.7 K has been demonstrated in the laboratory.

*Current TRL: 4*

*Resources to reach TRL 6: 2 years, \$500,000.*

**Cryogenic Thermal Transport Systems.** Detectors cooled to cryogenic temperatures often must be located large distances from a cooling source, such as a mechanical cryocooler or radiator. Conduction-based thermal links (such as thermal straps or conduction bars) can have large temperature gradients which reduces the efficiency of the cooling and be quite heavy. Cryogenic thermal transport systems are most beneficial as the transport length and/or heat load are increased. Beyond certain critical levels of thermal transport length and/or heat load, the weight, temperature gradients and parasitic heat loads of conduction-based heat transport devices becomes excessive. Two potential options for a cryogenic thermal transport system are the cryogenic capillary pumped loop (CCPL) and the cryogenic pumped gas loop (CPGL).

The CCPL is a two-phase evaporation/condensation loop that is miniaturized, lightweight, highly conductive, and diode acting (that is, the CCPL is inherently a thermal switch). Although CCPL functionality has been demonstrated both on the ground and in space (e.g., a nitrogen-filled CCPL flew as part of CRYOTSU on STS-95), there are significant technical hurdles that remain that require significant development. In particular, the ability for automatic cooldown of a large, distributed mass (like the optical bench cavity), needs to be developed. At 80 K, nitrogen is the perfect CCPL working fluid. At 190 K, ethane can be used. At 55 K, no working fluid is available, hence other transport options like the CPGL must be used.

*Current TRL: 5*

*Resources to reach TRL 6: 2 years, \$500,000.*

## **Lightweight composite optics and optical bench**

Reflectors fabricated from silicon carbide foam and graphite polycyanate ester composites are about one-half the weight of conventional glass optics. Prototype composite reflectors have been manufactured in sizes from 5-30 cm in diameter. The areal density of these reflectors ranges from 5.3-8.1 kg/m<sup>2</sup>. Surface figure accuracy of 1.2-1.5 microns has been demonstrated. In addition to being lightweight, composite optics have near-zero coefficients of thermal expansion. Thermally-stable optics are desirable for instruments such as TO3FPI that must be kept cold to eliminate background IR noise, since their shape and alignment is insensitive to temperature.

*Current TRL: 5*

*Resources to reach TRL 6: 1 year, \$200,000.*

## ACKNOWLEDGEMENTS

The instrument system conceptual design, including optical design, radiometric analysis, mechanical and thermal design, was completed by Swales Aerospace under Contract No. NAS5-32560, Task No. 560.

## ACRONYMS

CCPL	Cryogenic capillary pumped loop
CLIO	Circle to Line Interferometer Optical
CP	Conducting polymer
CPRL	Cryogenic pumped gas loop
CTE	Coefficient of thermal expansion
CTSU	Cryogenic thermal storage unit
FOV	Field of view
FPI	Fabry-Perot interferometer
FTS	Fourier transform spectrometer
LaRC	Langley Research Center
LSF	Line scan function
OES	Office of Earth Science
PZT	Piezoelectric transducer
SNR	Signal-to-noise ratio
THUNDER	Thin-layer composite unimorph ferroelectric device
TO3FPI	Tropospheric Ozone Fabry-Perot Interferometer
TRL	Technology readiness level
VCHP	Variable conductance heatpipe
ZPD	Zero path difference

## REFERENCES

- J. Bremer, T. D'Asto, E. Devine, J. Hunter, M. Krebs, K. Mehalick, B. Pasquale, "Tropospheric Ozone Instrument", Contract No. NAS5-32650, Task No. 2103-560, December 11, 1998.
- J. Fishman, C. E. Watson, J. C. Larsen, and J. A. Logan, "Distribution of Tropospheric Ozone Determined from Satellite Data", *J. Geophys. Res.*, Vol. 95, pp. 3599-3617, 1990.
- P. B. Hays, "Circle to Line Interferometer Optical System", *Appl. Opt.*, Vol. 29, pp. 1482-1489, 1990.
- P.B. Hays, V.J. Abreu, M.E. Dobbs, D.A. Gell, H.J. Grassl, and W.R. Skinner, "The High-Resolution Doppler Imager on the Upper Atmosphere Research Satellite", *J. Geophys. Res.*, Vol. 98, pp. 10713-10723, 1993.
- T.L. Killeen, B.C. Kennedy, P.B. Hays, S. D'Amico, and D.H. Ceckowski, "Image plane detector for the Dynamics Explorer Fabry-Perot interferometer", *Appl. Opt.*, pp. 3503-3513, 1983.
- W. R. Kuhn and J. London, "Infrared radiative cooling in the middle atmosphere (30-110 km)", *J. Atmos. Sci.*, Vol. 26, pp. 189-204, 1969.
- A. M. Larar, "The Feasibility of Tropospheric and Total Ozone Determination Using a Fabry-Perot Interferometer as a Satellite-Based Nadir-Viewing Atmospheric Sensor", Ph.D. thesis, Univ. of Michigan, 1993.
- A.M. Larar, P.B. Hays, and S.R. Drayson, "Global tropospheric and total ozone monitoring using a double-etalon Fabry-Perot interferometer. I: Instrument concept," *Appl. Opt.*, Vol. 37, pp. 4721-4731, 1998.
- A.M. Larar, and S.R. Drayson, "Global tropospheric and total ozone monitoring using a double-etalon Fabry-Perot interferometer. II: Feasibility analysis," *Appl. Opt.*, Vol. 37, pp. 4732-4743, 1998.
- A.M. Larar, W.B. Cook, and R.S. Lancaster, "Laboratory Prototype Double-Etalon Fabry-Perot Interferometer for Remotely Sensing Atmospheric Ozone: Atmospheric Measurements", *Society of Photo-Optical Instrumentation Engineers (SPIE) Proceedings*, Infrared Spaceborne Remote Sensing V conference, 1998b.
- L. S. Rothman, R. R. Gamache, A. Goldman, and L. R. Brown, R. A. Toth, H. M. Pickett, R. L. Poynter, J. -M. Flaud, C. Camy-Peyret, A. Barbe, N. Husson, C. P. Rinsland, and M. A. H. Smith, "The HITRAN database: 1986 edition", *Appl. Opt.*, Vol. 26, pp. 4058-4097, 1987.
- W.L. Smith, H.E. Revercomb, H.B. Howell, and H.M. Woolf, "HIS\_A Satellite Instrument to Observe Temperature and Moisture Profiles with High Vertical Resolution," in Fifth Conference on Atmospheric Radiation (American Meteorological Society, Boston) 1983.
- A. Volz, and D. Kley, "Evaluation of the Montsouris series of ozone measurements made in the nineteenth century", *Nature*, Vol. 332, pp. 240-242, 1988.
- J. Wang, "An Investigation on The Multiorder Fabry-Perot Interferometer as a Satellite-borne High Resolution Atmospheric Sounder", Ph.D. thesis, Univ. of Michigan, 1990.